# TGFB1 Induces Fetal Reprogramming and Enhances Intestinal Regeneration

Lei Chen[1,*], Xia Qiu[2], Abigail Dupre[2], Oscar Pellon-Cardenas[2], Xiaojiao Fan[1], Xiaoting Xu[1], Prateeksha Rout[2], Katherine D. Walton[3,4], Joseph Burclaff[5,6], Ruolan Zhang[1], Wenxin Fang[1], Rachel Ofer[2], Alexandra Logerfo[2], Kiranmayi Vemuri[2], Sheila Bandyopadhyay[7], Jianming Wang[8], Gaetan Barbet[9], Yan Wang[10], Nan Gao[7], Ansu O. Perekatt[11], Wenwei Hu[8], Scott T. Magness[5,6], Jason R. Spence[3,4,12], Michael P. Verzi[2,13,14,15,16,*]

[1]School of Life Science and Technology, Key Laboratory of Developmental Genes and Human Disease, Southeast University, Nanjing 210096, China
[2]Department of Genetics, Human Genetics Institute of New Jersey, Rutgers University, Piscataway, NJ 00854, USA
[3]Department of Internal Medicine, Gastroenterology, University of Michigan Medical School, Ann Arbor, MI 48109, USA
[4]Department of Cell and Developmental Biology, University of Michigan Medical School, Ann Arbor, MI 48109, USA
[5]Joint Department of Biomedical Engineering, University of North Carolina at Chapel Hill and North Carolina State University, NC 27695, USA
[6]Center for Gastrointestinal Biology and Disease, University of North Carolina at Chapel Hill School of Medicine, Chapel Hill, NC 27599, USA
[7]Department of Biological Sciences, Rutgers University, Newark 07102, NJ, USA
[8]Department of Radiation Oncology, Rutgers Cancer Institute of New Jersey, Rutgers University, New Brunswick, NJ 08903, USA
[9]Child Health Institute of New Jersey, Rutgers University, New Brunswick, NJ 08901, USA
[10]Center for Translation Medicine Research and Development, Shenzhen Institutes of Advanced Technology, Chinese Academy of Sciences, Shenzhen 518055, China
[11]Department of Chemistry and Chemical Biology, Stevens Institute of Technology, Hoboken, NJ 07030, USA
[12]Department of Biomedical Engineering, University of Michigan College of Engineering, Ann Arbor, MI 48109, USA
[13]Rutgers Cancer Institute of New Jersey, Rutgers University, New Brunswick, NJ 08903, USA
[14]Rutgers Center for Lipid Research, New Jersey Institute for Food, Nutrition & Health, Rutgers University, New Brunswick, NJ 08901, USA
[15]NIEHS Center for Environmental Exposures and Disease (CEED), Rutgers EOHSI Piscataway, NJ 08854, USA
[16]Lead contact

*Correspondence: leichen@seu.edu.cn; verzi@biology.rutgers.edu

## SUPPLEMENTARY FIGURE AND FIGURE LEGENDS

Figure S1

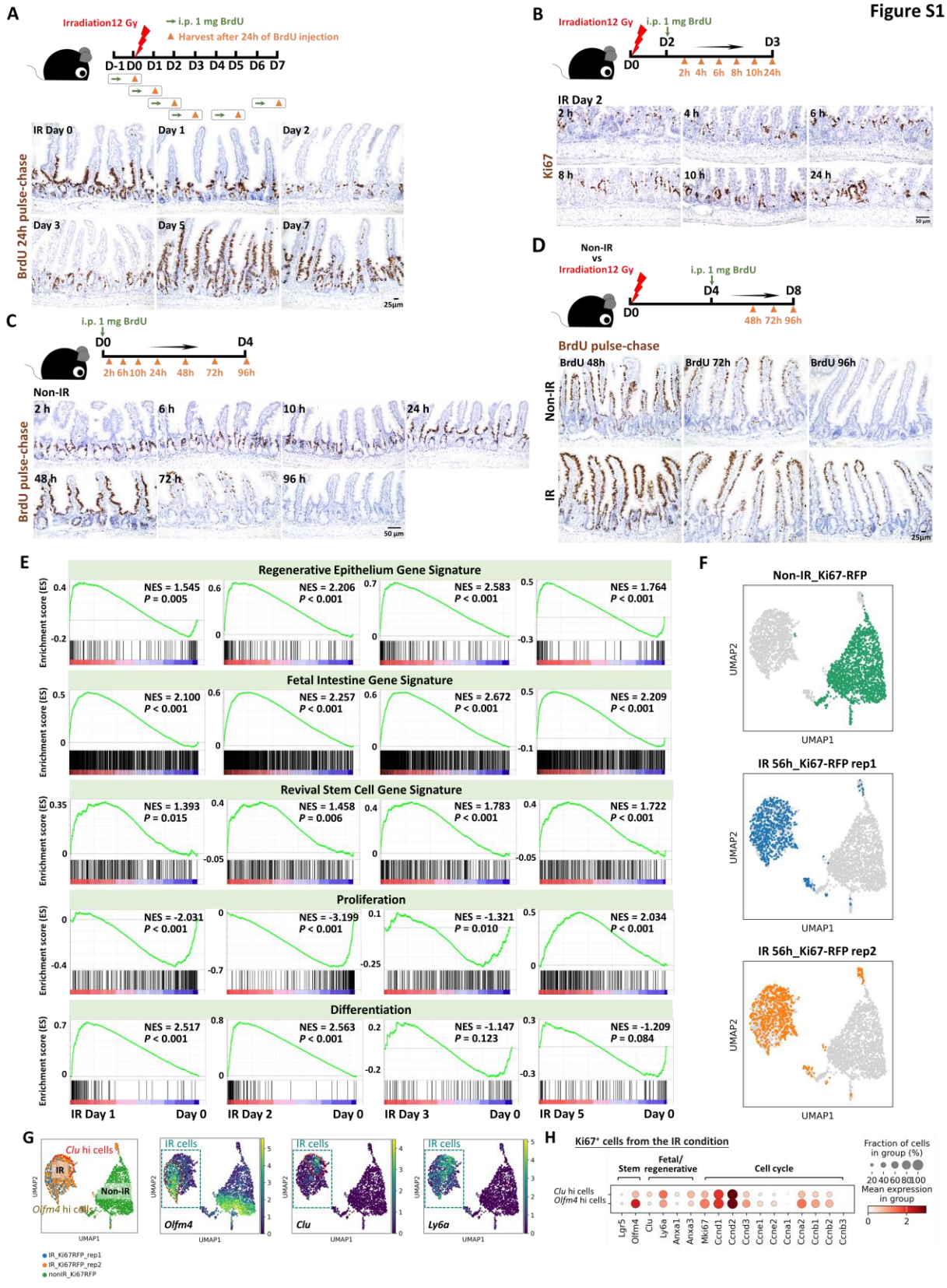

**Figure S1. Day 2 to Day 3 post-irradiation is a critical regeneration period of crypt cells, related to Figure 1. (A)** BrdU pulse-chase immunostaining of the intestine upon irradiation (representative of 3 biological replicates). Mice were injected with 1 mg of BrdU before or after irradiation. Intestines were collected after 24 hours of BrdU injection (see time-course details in the schematic of experimental design). **(B)** Immunostaining of Ki67 in the intestinal tissues of mice after 12 Gy irradiation. Ki67: proliferative marker, brown color; representative of 3 biological replicates. The schematic of experimental design was the same as BrdU experiment performed in **Figure 1B**. **(C)** BrdU pulse-chase immunostaining of the intestinal tissues collected from the non-IR control mice (representative of 3 biological replicates). For BrdU immunohistochemistry, mice were injected with 1 mg of BrdU. Intestinal tissues were harvested after 2, 6, 10, 24, 48, 72 and 96 hours of BrdU injection. **(D)** BrdU pulse-chase immunostaining of the intestinal tissues (representative of 3 biological replicates). Mice were injected with 1 mg of BrdU at Day 4 post-irradiation. Tissues were collected after 48, 72 and 96 hours of BrdU injection (see time-course details in the schematic of experimental design). BrdU positive cells are marked brown. Non-IR mice were used as controls. **(E)** GSEA examines expression changes in gene signatures of regenerative epithelium, fetal spheroid, revival stem cell, proliferation, and differentiation[1-5] at time points post-irradiation. Bulk RNA-seq was used in this analysis (GSE165157,[6] crypt cells, n=2 biological replicates per time-course, Kolmogorov-Smirnov test). **(F)** scRNA-seq reveals that sorted Ki67-RFP positive cells show different transcriptome profiles after 56 hours of irradiation compared to the non-IR controls. Number of cells in each condition was Non-IR Ki67-RFP positive cells: n=1739; IR 56h Ki67-RFP positive cells replicate 1: n=677; IR 56h Ki67-RFP positive cells replicate 2: n= 669. Ki67-RFP positive cells were isolated and sorted from crypt cells of *Mki67tm1.1Cle/J* mice after 56 hours of IR vs. non-IR control. scRNA-seq UMAP **(G)** and dot plots **(H)** reveal that *Clu* hi cells show relatively lower transcript levels of cell cycle genes than *Olfm4* hi cells in the sorted Ki67-RFP positive cells after 56 hours of irradiation.

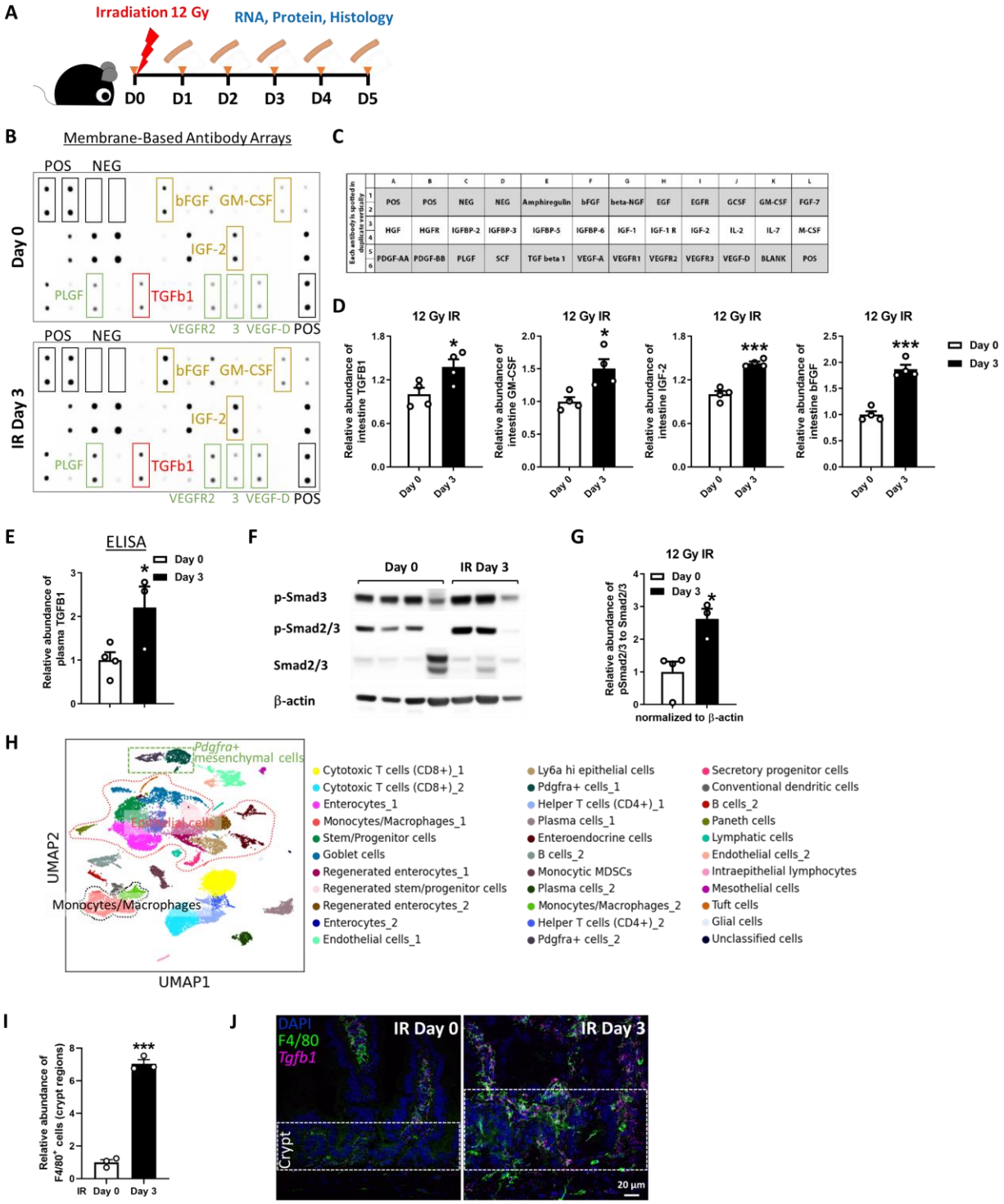


**Figure S2. TGFB signaling is activated in Day 3 irradiated mouse intestine, related to Figure 2. (A)** Schematics of IR time-course and sample collection for RNA, protein and histology. **(B-D)** Analysis of membrane-based antibody arrays. IGF-2 is reported to preprogram maturing macrophages (TGFB1 producers) to acquire oxidative phosphorylation-dependent anti-inflammatory properties.[7] On the other

hand, TGFB1 is known to enhance CM-CSF[8] and bFGF,[9] and we found TGFB1 and its related growth factors are all enriched in Day 3 intestine post-irradiation. Increased PLGF and VEGF were reported under pathologic situations, which are also observed in our study. **(D)** Quantification (n=2 independent experiments, 2 technical replicates per membrane, Student's t-test at $P < 0.001$*** and $P < 0.05$*). **(E)** Increased TGFB1 is observed in plasma at Day 3 post-irradiation compared to Day 0, as determined by ELISA (n=3-4 biological replicates, Student's t-test at $P < 0.05$*). **(F-G)** Western blot reveals that increased p-Smad3 and p-Smad2/3 levels (TGFB pathway) are detected in the intestine after 3 days of irradiation. Protein lysates were prepared from the 2 cm of duodenal fragments. **(G)** Quantification of western blot (n=3-4 biological replicates, Student's t-test at $P < 0.05$*). TGFB1: Transforming growth factor beta 1; bFGF: Basic fibroblast growth factor; GM-CSF: Granulocyte-macrophage colony-stimulating factor; IGF-2: insulin-like growth factor; PLGF: Placental growth factor; VEGF: Vascular endothelial growth factor. **(H)** Identified cell populations of intestinal scRNA-seq data following mouse irradiation at days 0, 1, 3, 7, and 14, as shown in **Figure 2E** (GSE165318, n=3-4 biological replicates per time-course). **(I)** Quantification of F4/80 positive cells in the crypt regions (n=3 biological replicates, Student's t-test at $P < 0.001$***). **(J)** High magnification RNAscope images shows localized *Tgfb1* transcripts relative to immunostaining signal from F4/80 (representative of 3 biological replicates).

**Figure S3**

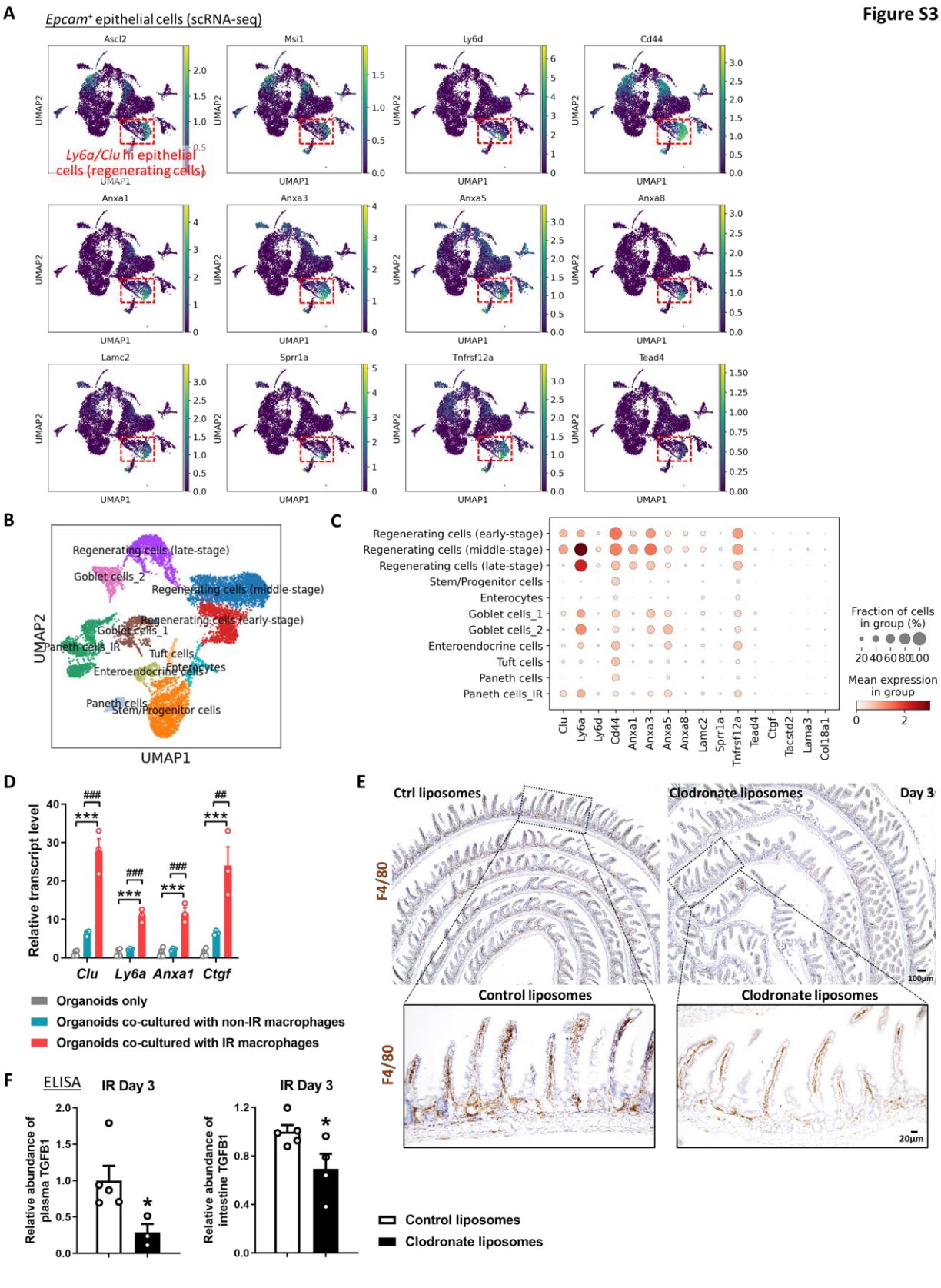
A
Epcam+ epithelial cells (scRNA-seq)
Ascl2
Msi1
Ly6d
Cd44
Ly6a/Clu hi epithelial cells (regenerating cells)
Anxa1
Anxa3
Anxa5
Anxa8
Lamc2
Sprr1a
Tnfrsf12a
Tead4
UMAP1
UMAP2
B
Regenerating cells (late-stage)
Goblet cells_2
Regenerating cells (middle-stage)
Regenerating cells (early-stage)
Goblet cells_1
Paneth cells_IR
Tuft cells
Enterocytes
Enteroendocrine cells
Paneth cells
Stem/Progenitor cells
C
Regenerating cells (early-stage)
Regenerating cells (middle-stage)
Regenerating cells (late-stage)
Stem/Progenitor cells
Enterocytes
Goblet cells_1
Goblet cells_2
Enteroendocrine cells
Tuft cells
Paneth cells
Paneth cells_IR
Clu
Ly6a
Ly6d
Cd44
Anxa1
Anxa3
Anxa5
Anxa8
Lamc2
Sprr1a
Tnfrsf12a
Tead4
Ctgf
Tacstd2
Lama3
Col18a1
Fraction of cells in group (%)
20 40 60 80 100
Mean expression in group
0
2
D
Relative transcript level
Clu
Ly6a
Anxa1
Ctgf
Organoids only
Organoids co-cultured with non-IR macrophages
Organoids co-cultured with IR macrophages
E
Ctrl liposomes
Clodronate liposomes
Day 3
F4/80
100μm
Control liposomes
Clodronate liposomes
20μm
F
ELISA
IR Day 3
Relative abundance of plasma TGFB1
Relative abundance of intestine TGFB1
Control liposomes
Clodronate liposomes

**Figure S3. Fetal/regenerative genes are highly enriched during regeneration, related to Figure 3. (A)** scRNA-seq of mouse intestines across a time-course post-irradiation (GSE165318). Of all the epithelial cells in the dataset (marked by *Epcam* expression in **Figure 3B**), regenerating cells expressing *Tgfbr2* are also highly enriched in transcript levels of reserve stem cell genes and fetal/regenerative marker genes. **(B-C)** *Msi1-CreERT2; R26-mTmG* mice were treated with tamoxifen for 15 hours, and *Msi1* positive GFP cells were sorted for scRNA-seq. Identified cell populations **(B)** of intestinal scRNA-seq data following mouse irradiation at days 0, 1, 2, 3, and 5 (GSE145866[10]). Fetal/regenerative transcripts **(C)** are highly enriched in these regenerating cells. **(D)** qRT-PCR indicates that expression of fetal/regenerative marker genes increases in organoids co-cultured with primary intestinal macrophages isolated from mice at 3 days post-IR compared to organoids co-cultured with non-IR control macrophages or organoids only. All the data are presented as mean ± SEM (n=3-4 independent cultures). Statistical comparisons were performed using one-way ANOVA followed by Tukey's multiple comparisons test at $P < 0.001$*** (Organoids co-cultured with IR macrophages vs Organoids only); $P < 0.001^{\#\#\#}$ or $P < 0.01^{\#\#}$ (Organoids co-cultured with IR macrophages vs Organoids co-cultured with non-IR macrophages). **(E-F)** Monocytes/Macrophages were depleted using clodronate-containing liposomes (see schematic of experimental design in **Figure 3F**). Immunostaining **(E)** was performed to confirm reduction in F4/80 expressing cells upon treatment. Reduced levels of TGFB1 are observed in the plasma and intestine upon treatment of clodronate liposomes compared to treatment with control liposomes, as evidenced by ELISA **(F)**. Plasma and duodenal fragments were collected 3 days post-irradiation (n=3-5 biological replicates, Student's t-test at $P < 0.05$*).

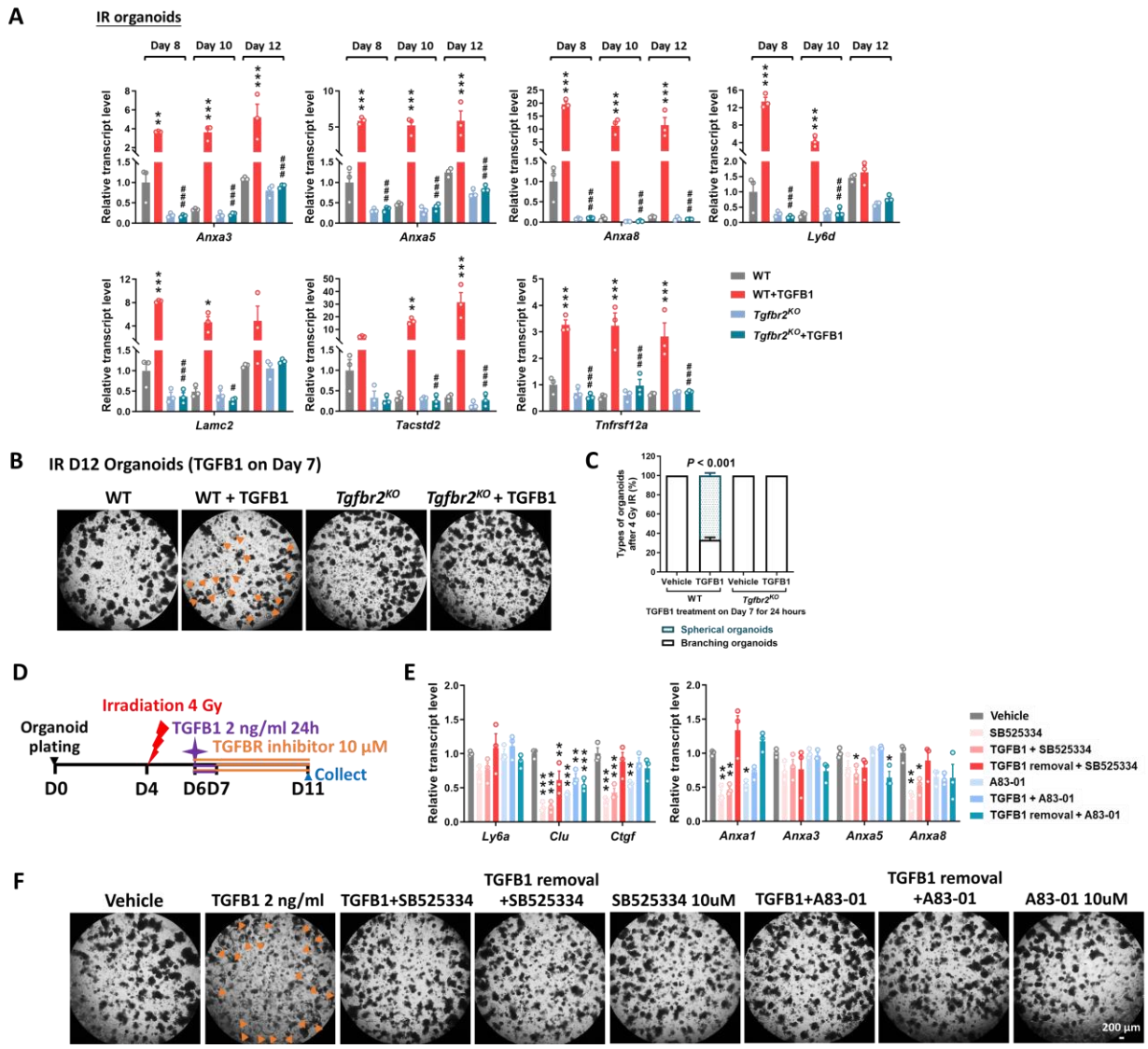


**Figure S4. Inactivation of *Tgfbr2* abolishes TGFB1-induced spheroid morphology and fetal/regenerative gene signatures, related to Figure 4. (A)** qRT-PCR indicates that expression of regeneration marker genes increases within 24 hours and remains elevated for at least 5 days post-TGFB1 treatment in organoids post-irradiation. This induction is dependent on *Tgfbr2*. Schematic of experimental design of qRT-PCR for panel A is depicted in **Figure 4F**. All the data are presented as mean ± SEM (n=3 independent organoid cultures). Statistical comparisons were performed using one-way ANOVA followed by Tukey's multiple comparisons test at $P < 0.001$***, $P < 0.01$** or $P < 0.05$* (WT+TGFB1 vs WT); $P < 0.001^{###}$, $P < 0.01^{##}$ or $P < 0.05^{#}$ (*Tgfbr2*$^{KO}$+TGFB1 vs WT+TGFB1). **(B-C)** Loss of *Tgfbr2* abolishes TGFB1 induced spheroid morphology (orange arrows, n=3 independent organoid cultures). **(B)** Representative images. **(C)** Quantification. Statistical comparisons were performed using one-way ANOVA followed by Dunnett's post at $P < 0.001$. Schematic of experimental design for panels B-C is in **Figure 4F**. These findings were corroborated by adding TGFB receptor inhibitors **(D-F)**. **(D)** Schematic of intervention experiment using TGFB receptor inhibitors. Primary intestinal organoids were exposed to 4 Gy of irradiation on Day 4, followed by TGFB1 treatment (2 ng/ml) on Day 6 for 24 hours.

TGFB receptor inhibitor, 10 μM SB525334 or A83-01, was added at the same time with TGFB1 treatment, or added after removal of TGFB1, or added without TGFB1 pre-treatment. The corresponding intervention continued until Day 11. Organoids were imaged on Day 11, and then collected for qRT-PCR. **(E)** Presence of TGFB receptor inhibitors suppresses TGFB1-induced expression of fetal/regenerative genes. Transcript levels relative to vehicle, and statistical comparisons were performed using one-way ANOVA followed by Dunnett's post at $P < 0.001$***, $P < 0.01$** or $P < 0.05$* (n=3 independent organoid cultures). All the qRT-PCR data are presented as mean ± SEM. **(F)** TGFB receptor inhibitors abolish TGFB1-induced spheroid morphology (orange arrows, n=3 independent organoid cultures).

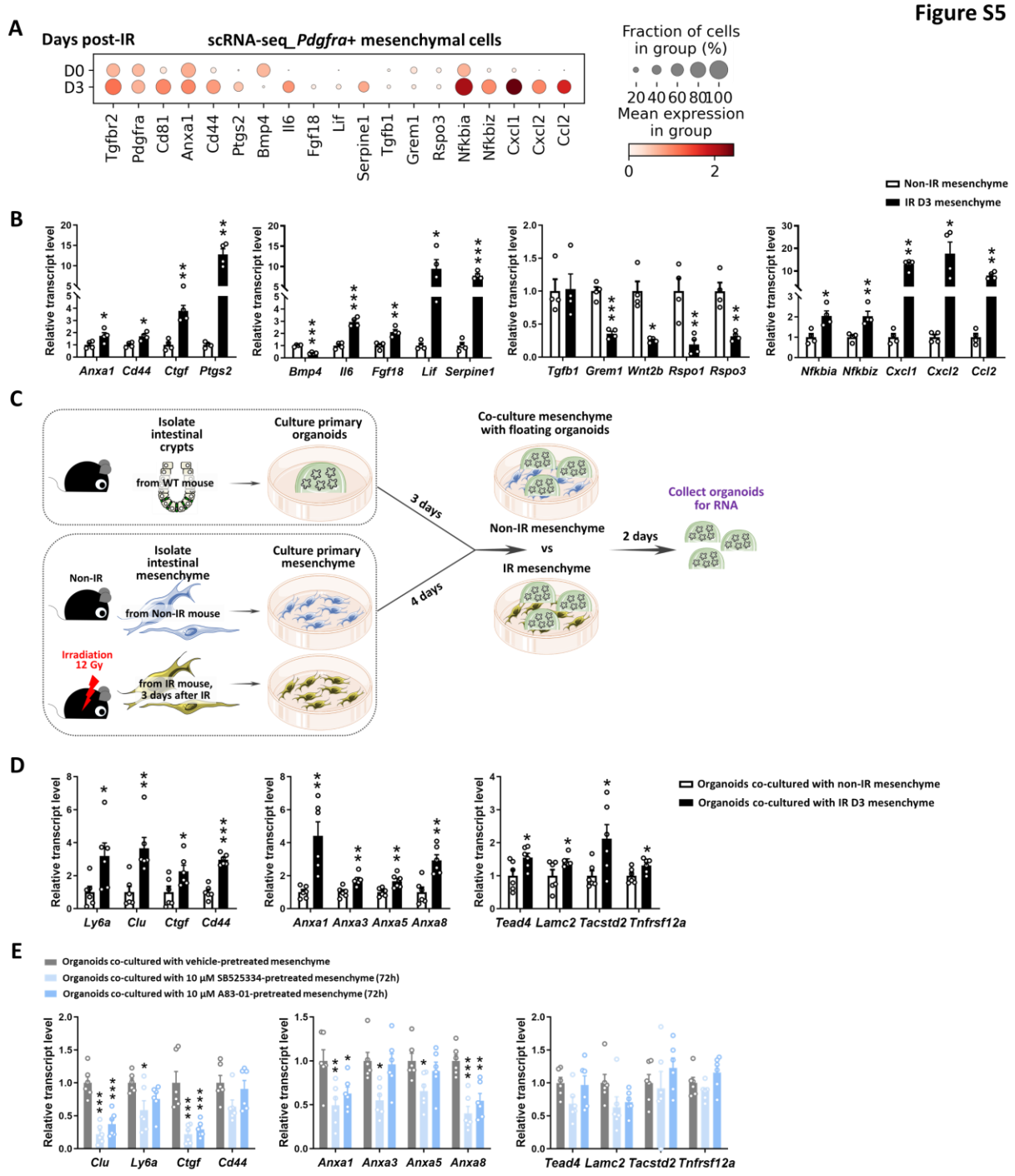


**Figure S5. Mesenchyme isolated from mice post-irradiation promotes fetal-like gene signatures of intestinal organoids, related to Figure 5. (A-B)** Cultured mesenchymal cells isolated from mice with or without irradiation harbor similar features of cells isolated from primary *Pdgfra* positive mesenchymal cells, as evidenced by scRNA-seq dot plots **(A)** of *Pdgfra* positive mesenchyme cell cluster (primary cells, GSE165318) and qRT-PCR **(B)** of cultured mesenchyme (n=4 independent mesenchyme cultures with 2 different primary cell lines). **(C)** Schematic of co-culture experimental design. Intestinal mesenchymal cells were isolated from mice with or without irradiation (12 Gy, 3 days post-IR) and cultured for 4 days.

They were then overlaid with Day 3 primary organoids in matrigel bubbles for another 2 days. Co-cultured organoids were collected as floating matrix bubbles for qRT-PCR. **(D)** qRT-PCR reveals that compared to the non-IR condition, mesenchyme isolated from mice post-irradiation shows stronger induction of fetal/regenerative gene expression in co-cultured organoids (n=6 independent organoid cultures with 2 different cell lines of mesenchyme and 3 different cell densities). The qRT-PCR data are presented as mean ± SEM (Student's t-test at $P < 0.001$***, $P < 0.01$** or $P < 0.05$* for panels B and D). **(E)** Mesenchyme pre-treated with TGFBR inhibitors suppresses fetal-like gene signatures of co-cultured intestinal organoids. Passaged intestinal mesenchyme cells were pre-treated with vehicle or TGFBR inhibitors for 3 days, and then co-cultured with Day 3 primary organoids for 2 days (similar procedure as shown in **Figure 5D**). Co-cultured organoids were collected for qRT-PCR (n=6 independent organoid cultures with 2 different cell densities of mesenchyme). TGFBR inhibitors were removed during co-culture. Transcript levels relative to vehicle control, and statistical comparisons were performed using one-way ANOVA followed by Dunnett's post at $P < 0.001$***, $P < 0.01$** or $P < 0.05$*.

Figure S6

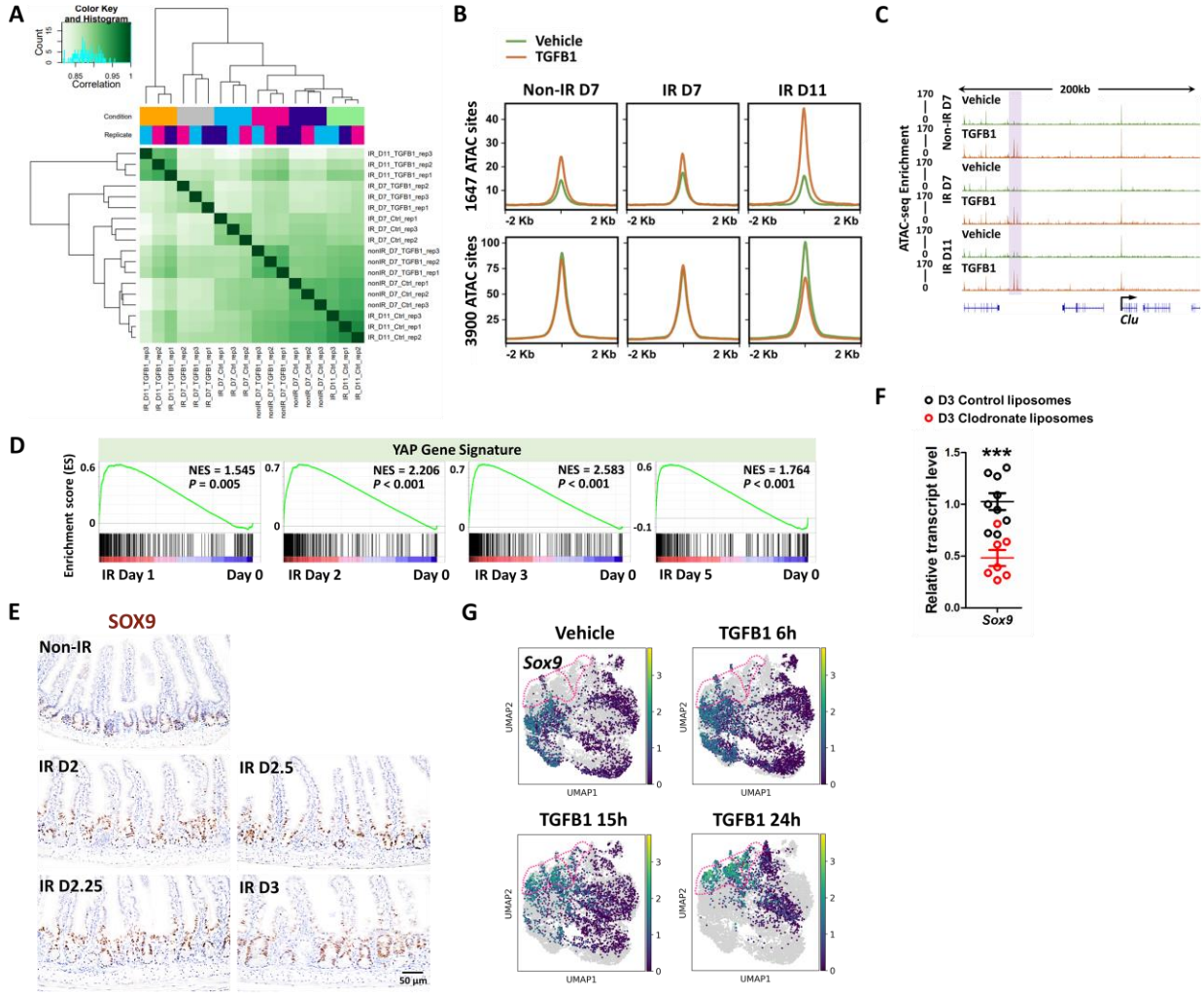


**Figure S6. TGFB1 activates intestinal YAP and SOX9 regenerative programs, related to Figure 6. (A)** ATAC-seq correlation heatmap of organoids upon TGFB1 treatment (DiffBind package, n=3 independent organoid cultures, at MACS2 called peaks of $q < 0.05$). The experimental design is the same as bulk RNA-seq and shown in **Figure 4A**. **(B)** Average signal of ATAC-seq in accessible chromatin regions of vehicle or TGFB1 treated organoids (Differential ATAC-seq regions defined in **Figure 6A**, Diffbind FDR < 0.01). **(C)** Examples of genes located at ATAC-seq enriched regions of TGFB1-treated organoids using IGV. **(D)** GSEA reveals gene signatures of elevated YAP signaling[11] post-irradiation, using a bulk RNA-seq of an IR time-course data set (GSE165157[6], crypt cells, n=2 biological replicates per time-course, Kolmogorov-Smirnov test). **(E)** Intestinal immunostaining of SOX9 from day 2 to day 3 post-IR vs. non-IR (brown color; representative of 3 biological replicates). **(F)** Depletion of monocytes/macrophages (main cell sources of TGFB1 secretion) results in a downregulation of *Sox9*, as evidenced by qRT-PCR (n=7-9 biological replicates, duodenal fragments, Student's t-test at $P < 0.001$***). **(G)** scRNA-seq UMAP plots indicate that TGFB1 induces *Clu*-expressing cells that highly express *Sox9* (shown within pink dotted line, defined in **Figure 4K**). Number of cells in each condition was Vehicle: n= 2815; TGFB1 6h: n= 4071; TGFB1 15h: n= 2788; TGFB1 24h: n=2177.

Figure S7

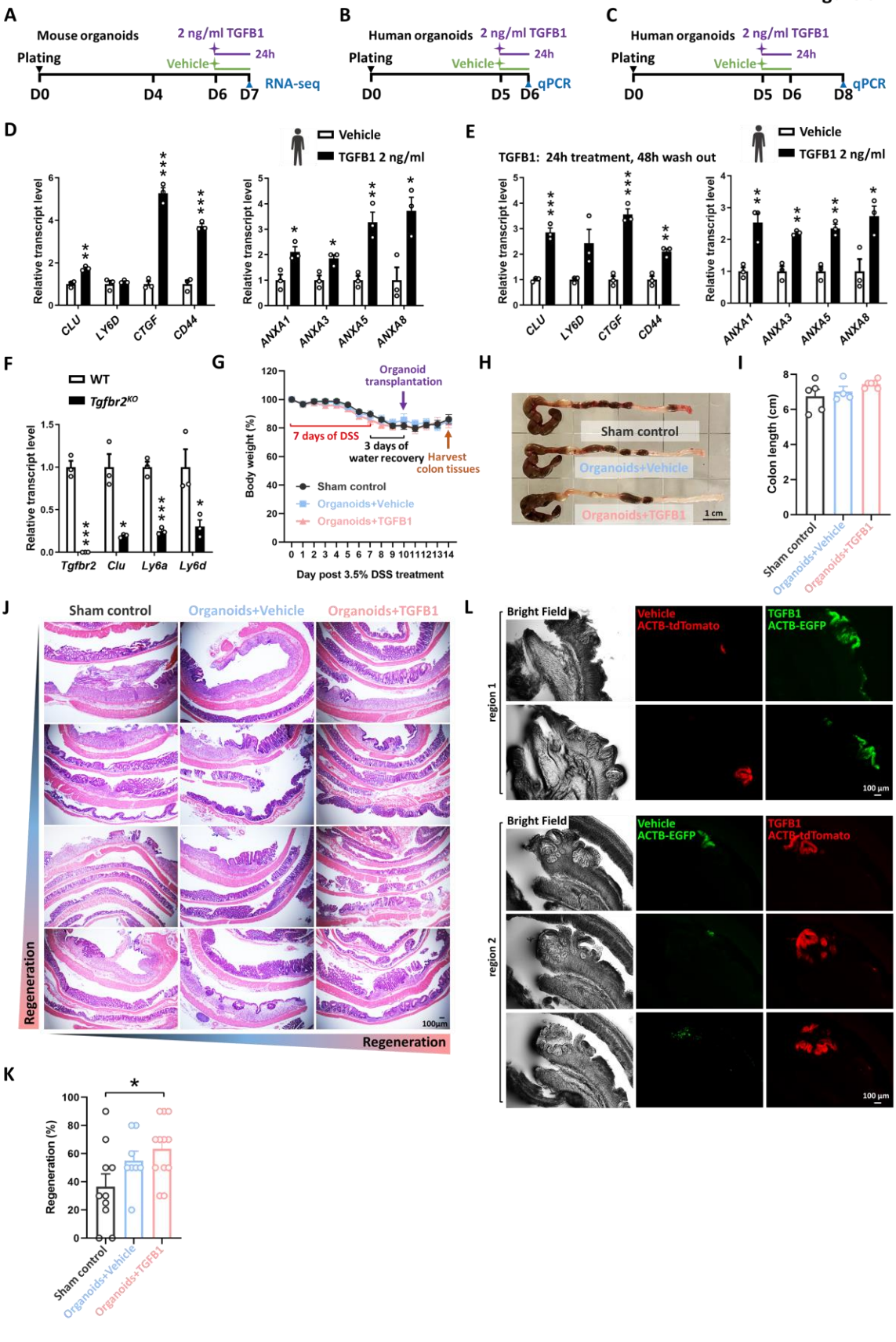
A
Mouse organoids
Plating
2 ng/ml TGFB1
Vehicle
24h
RNA-seq
D0
D4
D6
D7
B
Human organoids
Plating
2 ng/ml TGFB1
Vehicle
24h
qPCR
D0
D5
D6
C
Human organoids
Plating
2 ng/ml TGFB1
Vehicle
24h
qPCR
D0
D5
D6
D8
D
Vehicle
TGFB1 2 ng/ml
Relative transcript level
CLU
LY6D
CTGF
CD44
ANXA1
ANXA3
ANXA5
ANXA8
E
TGFB1: 24h treatment, 48h wash out
Vehicle
TGFB1 2 ng/ml
Relative transcript level
CLU
LY6D
CTGF
CD44
ANXA1
ANXA3
ANXA5
ANXA8
F
WT
Tgfbr2KO
Relative transcript level
Tgfbr2
Clu
Ly6a
Ly6d
G
Organoid transplantation
7 days of DSS
3 days of water recovery
Harvest colon tissues
Body weight (%)
Sham control
Organoids+Vehicle
Organoids+TGFB1
Day post 3.5% DSS treatment
H
Sham control
Organoids+Vehicle
Organoids+TGFB1
1 cm
I
Colon length (cm)
Sham control
Organoids+Vehicle
Organoids+TGFB1
J
Sham control
Organoids+Vehicle
Organoids+TGFB1
Regeneration
Regeneration
100μm
K
Regeneration (%)
Sham control
Organoids+Vehicle
Organoids+TGFB1
L
Bright Field
Vehicle
ACTB-tdTomato
TGFB1
ACTB-EGFP
region 1
100 μm
Bright Field
Vehicle
ACTB-EGFP
TGFB1
ACTB-tdTomato
region 2
100 μm

**Figure S7. TGFB1 pre-treated organoids transplant more efficiently in DSS-damaged colon, related to Figure 7. (A)** Schematic for the bulk RNA-seq experimental design of non-IR mouse organoids. **(B-E)** TGFB1-induced fetal/regenerative gene signatures are conserved in adult human duodenal organoid cultures. qRT-PCR indicates that expression of regeneration marker genes increases and remains elevated for at least 3 days post-TGFB1-treatment in adult human duodenal organoid cultures. TGFB1 treatment was performed for a 24-hour window either **(B, D)** 24 hours or **(C, E)** 72 hours before collection of cells. Human organoids were treated with TGFB1 on Day 5 (n=3 independent organoid cultures, Student's t-test at $P < 0.001$***, $P < 0.01$** or $P < 0.05$*). All the qRT-PCR data are presented as mean ± SEM. **(F)** To inactivate*Tgfbr2*, *Tgfbr2f/f*; *Villin-Cre*$^{ERT2}$ mice were injected with tamoxifen for 4 consecutive days, and harvested 4 days after the first injection for primary organoid culture. Littermate controls were injected with vehicle. WT and *Tgfbr2*$^{KO}$ organoids were collected on Day 7. qRT-PCR reveals that fetal/regenerative genes are suppressed in intestinal organoids upon loss of *Tgfbr2* (n=3 independent organoid cultures, Student's t-test at $P < 0.001$***, $P < 0.01$** or $P < 0.05$*). **(G-K)** Comparison of DSS-treated mice receiving transplantation of vehicle-treated organoids or TGFB1-treated organoids or sham controls. All the data are presented as mean ± SEM (n=4-6 biological replicates). Statistical comparisons were performed using one-way ANOVA followed by Dunnett's post at $P < 0.05$*. **(G)** Body weight of mice treated with DSS in organoid transplantation experiment. NOD mice were treated with 3.5% DSS for 7 days. After 3 days of water recovery, organoid transplantation was performed and colon tissues were harvested 4 days after organoid transplant. **(H)** Representative colon images. **(I)** Quantification of colon length. **(J)** Representative H&E images of colon from different biological replicates. **(K)** Percentage of colonic area populated by regenerating epithelium from different treatment groups. Swiss rolls were generated from colon tissues, cut in half, and sectioned. The percentage of the distal colon covered by regenerating epithelium was measured on a section from each side of the colon for each mouse. **(L)** TGFB1 pre-treatment enhances organoid engraftment in DSS-treated mice. Examples of representative regions. Consecutive cryosections that represent the same colonization event were counted as one region. 21 organoid-colonized regions were found from 5 mice.

## REFERENCES


1. Ayyaz, A., Kumar, S., Sangiorgi, B., Ghoshal, B., Gosio, J., Ouladan, S., Fink, M., Barutcu, S., Trcka, D., Shen, J., et al. (2019). Single-cell transcriptomes of the regenerating intestine reveal a revival stem cell. Nature *569*, 121-125. 10.1038/s41586-019-1154-y.
2. Merlos-Suarez, A., Barriga, F.M., Jung, P., Iglesias, M., Cespedes, M.V., Rossell, D., Sevillano, M., Hernando-Momblona, X., da Silva-Diz, V., Munoz, P., et al. (2011). The intestinal stem cell signature identifies colorectal cancer stem cells and predicts disease relapse. Cell stem cell *8*, 511-524. 10.1016/j.stem.2011.02.020.
3. Mustata, R.C., Vasile, G., Fernandez-Vallone, V., Strollo, S., Lefort, A., Libert, F., Monteyne, D., Perez-Morga, D., Vassart, G., and Garcia, M.I. (2013). Identification of Lgr5-independent spheroid-generating progenitors of the mouse fetal intestinal epithelium. Cell Rep *5*, 421-432. 10.1016/j.celrep.2013.09.005.
4. Wang, Y., Chiang, I.L., Ohara, T.E., Fujii, S., Cheng, J., Muegge, B.D., Ver Heul, A., Han, N.D., Lu, Q., Xiong, S., et al. (2019). Long-Term Culture Captures Injury-Repair Cycles of Colonic Stem Cells. Cell *179*, 1144-1159 e1115. 10.1016/j.cell.2019.10.015.
5. Yui, S., Azzolin, L., Maimets, M., Pedersen, M.T., Fordham, R.P., Hansen, S.L., Larsen, H.L., Guiu, J., Alves, M.R.P., Rundsten, C.F., et al. (2018). YAP/TAZ-Dependent Reprogramming of Colonic

Epithelium Links ECM Remodeling to Tissue Regeneration. Cell stem cell *22*, 35-49 e37. 10.1016/j.stem.2017.11.001.

6. Qu, M., Xiong, L., Lyu, Y., Zhang, X., Shen, J., Guan, J., Chai, P., Lin, Z., Nie, B., Li, C., et al. (2021). Establishment of intestinal organoid cultures modeling injury-associated epithelial regeneration. Cell Res *31*, 259-271. 10.1038/s41422-020-00453-x.
7. Du, L., Lin, L., Li, Q., Liu, K., Huang, Y., Wang, X., Cao, K., Chen, X., Cao, W., Li, F., et al. (2019). IGF-2 Preprograms Maturing Macrophages to Acquire Oxidative Phosphorylation-Dependent Anti-inflammatory Properties. Cell Metab *29*, 1363-1375 e1368. 10.1016/j.cmet.2019.01.006.
8. Celada, A., and Maki, R.A. (1992). Transforming growth factor-beta enhances the M-CSF and GM-CSF-stimulated proliferation of macrophages. Journal of immunology *148*, 1102-1105.
9. Pertovaara, L., Saksela, O., and Alitalo, K. (1993). Enhanced bFGF gene expression in response to transforming growth factor-beta stimulation of AKR-2B cells. Growth Factors *9*, 81-86. 10.3109/08977199308991584.
10. Sheng, X., Lin, Z., Lv, C., Shao, C., Bi, X., Deng, M., Xu, J., Guerrero-Juarez, C.F., Li, M., Wu, X., et al. (2020). Cycling Stem Cells Are Radioresistant and Regenerate the Intestine. Cell Rep *32*, 107952. 10.1016/j.celrep.2020.107952.
11. Gregorieff, A., Liu, Y., Inanlou, M.R., Khomchuk, Y., and Wrana, J.L. (2015). Yap-dependent reprogramming of Lgr5(+) stem cells drives intestinal regeneration and cancer. Nature *526*, 715-718. 10.1038/nature15382.